SPATIO TEMPORAL CHANGE DETECTION OF URBANIZATION

A PROJECT REPORT

URBANIZATION OF SOUTH 24 PARAGANAS

Submitted by

ABHISHEK ROY
ABHISHEK BANIK
SAMPRIT DAS
MONODIP BISWAS

Supervised by

Ms. DIPANWITA GHOSH

In partial fulfillment for the award of the degree

Of

BACHELOR OF TECHNOLOGY

IN

INFORMATION TECHOLOGY

MAULANA ABUL KALAM AZAD UNIVERSITY OF TECHNOLOGY,
XG5V+27R, Haringhata Farm, West Bengal 741249

BONAFIDE CERTIFICATE

Certified that this project report **"SPATIO TEMPORAL CAHNGE DETECTION OF URBANIZATION"** is the bonafide work of **"ABHISHEK ROY, SAMPRIT DAS, MONODIP BISAWS, ABHISHEK BANIK"** who carried out the project work under my supervision.

Signature of the Head of the Department

Signature of the Supervisor

SOMDUTTA CHAKRABORTY

HEAD OF THE DEPARTMENT

Ms.DIPANWITA GHOSH

SUPERVISOR

Signature of External Examiner:

ACKNOWLEDGEMENT

We would like to express our deepest appreciation to all those who provided us the possibility to complete this project report. A special gratitude we give to our final year project mentor**, Ms. DIPANWITA GHOSH**, whose contribution in stimulating suggestions and encouragement, helped us to coordinate our project, especially in writing this report.

Many thanks to the mentor of our project, **Ms. DIPANWITA GHOSH,** who has invested his full effort in guiding the team in achieving the goal. We appreciate the guidance given by other supervisors as well as the panels, especially in our project presentation that has improved our presentation skills thanks to their comments and advice.

ABHISEK ROY

MONODIP BISWAS

SAMPRIT DAS

ABHISHEK BANIK

TABLE OF CONTENTS

Abstract

This research examines the spatio-temporal transformations in urbanization within Newtown, North 24 Parganas, India, through the utilization of Landsat satellite imagery spanning 2013 and 2023. The primary objective is to offer valuable insights for effective land planning decisions by identifying notable positive and negative changes in the area. The analysis of the satellite images reveals several significant trends. Firstly, there has been a considerable rise in habitation, indicating the expansion of urban areas and a remarkable influx of residents into Newtown. This demographic shift is further supported by an estimated residential population surpassing one million as of April 2018, accompanied by an additional floating population of 0.5 million. Secondly, the conversion of previously unused or underutilized wasteland has resulted in a reduction in such land. This conversion signifies a substantial demand for land due to urban development in the region and highlights the pressures on available land resources. Thirdly, there has been a decline in the extent of agricultural land, indicating its conversion for non-agricultural purposes. This trend likely reflects the necessity to accommodate the demands of urbanization and the growing population. Lastly, the most noteworthy change observed is the decrease in the presence of water bodies alongside the increase in habitation. This finding suggests the encroachment or filling of natural features such as lakes, ponds, or rivers to facilitate the development of urban infrastructure. In conclusion, this study provides valuable insights into the changes in land use and urbanization patterns within Newtown North 24 Parganas, over the examined decade. The findings aim to inform policymakers and land planners about the spatial and temporal dynamics of the region, enabling informed decisions regarding resource allocation, infrastructure planning, and sustainable urban growth. Additionally, the study highlights the robustness of land cover mapping by reporting the overall classification accuracy achieved in the designated area. Accurate and up-to-date information on urbanization trends is crucial for effective urban planning and decision-making. The process of urbanization has undergone rapid and extensive transformation in recent decades, resulting in significant alterations in the spatial and temporal patterns of urban areas globally. Understanding and monitoring these spatio-temporal changes in urbanization are crucial for effective urban planning, resource management, and sustainable development. This comprehensive review paper intends to provide an overview of the key factors driving the dynamics of urbanization and the methodologies employed to analyze spatio-temporal changes in urban areas. The paper commences by discussing the drivers of urbanization, encompassing population growth, economic development, technological advancements, and social factors. It emphasizes the importance of considering both the natural and human-induced factors that influence patterns of urbanization at various scales. Next, the review explores the methodologies and data sources commonly utilized to analyze spatio-temporal changes in urban areas. Remote sensing, geographic information systems (GIS), and spatial analysis techniques are examined, underscoring their capabilities in mapping and monitoring urban growth, changes in land use, and urban sprawl. Additionally, the integration of satellite imagery, aerial photography, and ground-based surveys is explored to provide a comprehensive understanding of the dynamics of urbanization. The review further examines the spatial patterns and trends of urbanization across different regions, highlighting the variations in rates of urban growth, land consumption, and urban form. It emphasizes the significance of studying urbanization at multiple scales, ranging from local neighborhoods to regional and global contexts, in order to capture the diverse dynamics and impacts of urbanization processes. Furthermore, the report discusses the consequences of rapid urbanization, including environmental degradation, loss of agricultural land, increased energy consumption, and social inequalities. It emphasizes the need for sustainable urban planning and policy interventions to address these challenges and promote inclusive and resilient urban development.

Finally, the review concludes by identifying research gaps and future directions for studying spatio-temporal changes in urbanization. It highlights the potential

Chapter 1

1. Introduction

The increase in population and human activities has resulted in a heightened demand for limited water resources, agricultural land, forests, urban areas, and industrial development. However, the expansion of human settlements and the need for additional land for various purposes has led to a decline in the quality and quantity of natural resources. Understanding the spatio-temporal changes in land use is essential for numerous applications, including hydrological and climate modeling, as well as informing policymakers about regional climate dynamics, water resource availability, and biochemical cycles in terrestrial ecosystems. To facilitate the exploration of these changes, the Earth Explorer interface, developed by the United States, provides an online search and browsing platform that integrates satellite and remote sensing inventories. Leveraging the capabilities of Google Maps, users can efficiently navigate and zoom in or out, and even access Google Street View to obtain a realistic visual representation of selected locations. This interface offers the convenience of downloading high-resolution satellite images of New Town by zooming in on the desired area of interest. Additionally, the analysis of spatio-temporal data encompasses multiple driving factors, including biophysical conditions, economic activities, and other influential variables. Incorporating geographic and temporal dimensions enhances the representation of these factors, enabling a comprehensive understanding of the impact of human activities on the natural environment. In summary, spatio-temporal data analysis is a sophisticated technique that is gaining momentum in the analysis of vast databases containing spatial and temporal information. By unraveling the dynamics of land use changes, this approach provides valuable insights for informed decision-making, sustainable resource management, and addressing the environmental consequences of human influences.

Chapter 2

2. Study Area

The study area that has been selected is the New Town of North 24 Parganas district and is a part of New Town Kolkata Development, as this comprises a blend of residential developments, commercial cum retail complexes, corporate parks and institutional entities.

State Districts

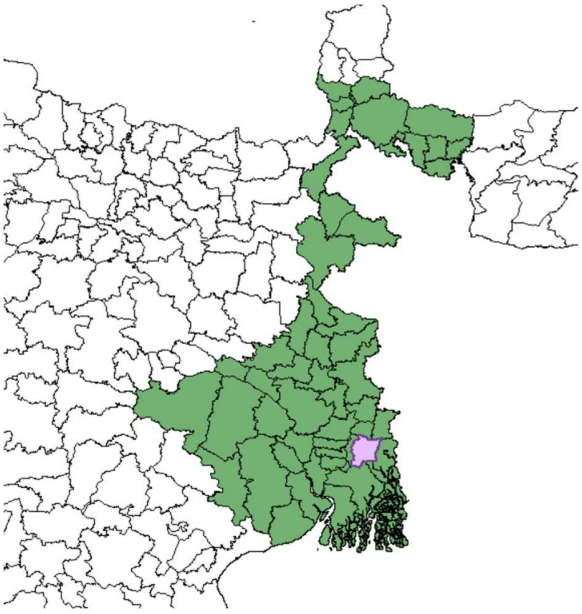

Dividing more into Subdistricts

The Area of Interest

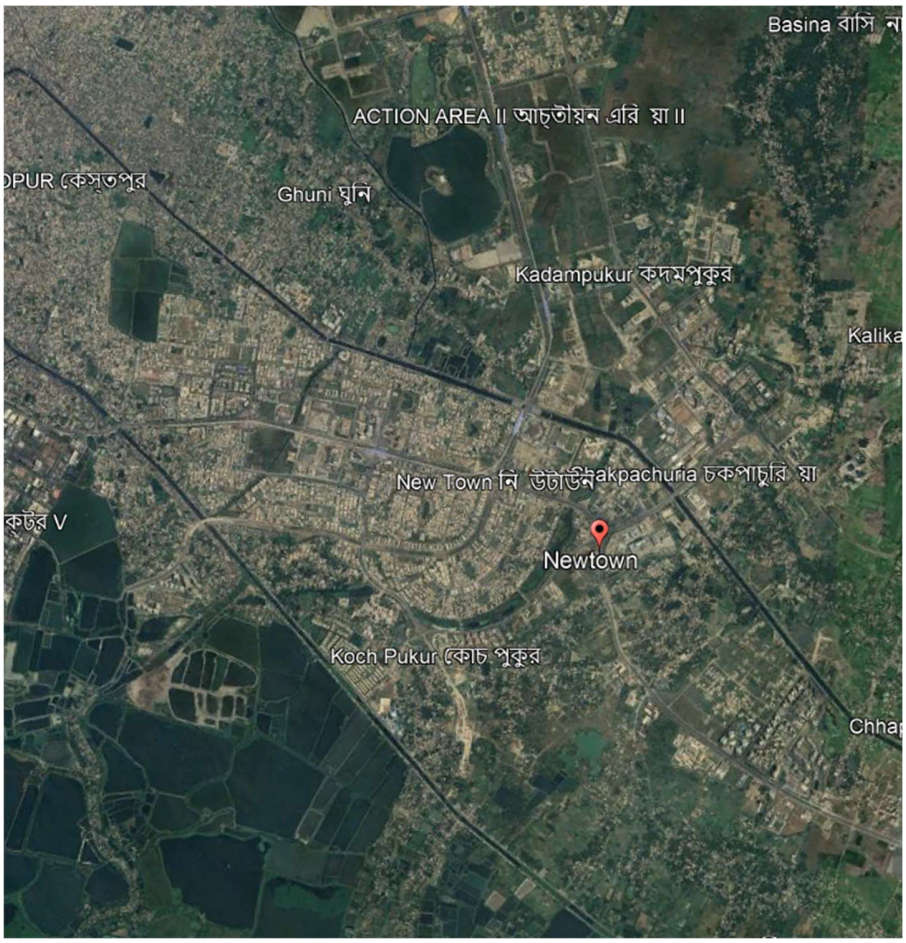

The Satellite view of the region we are working on

Chapter 3

3.1. Literary Survey

Urbanization is a dynamic process that involves the expansion and transformation of cities and towns, leading to significant changes in land use and land cover. Detecting and understanding spatio-temporal changes in urban areas is crucial for effective urban planning, resource management, and environmental assessment. In recent years, researchers have employed various methods and techniques to detect and analyze urbanization patterns and trends. This literature survey provides an overview of some key studies and approaches related to spatio-temporal change detection of urbanization.

Remote Sensing-Based Approaches: Remote sensing techniques, particularly the use of satellite imagery, have been widely employed for monitoring urbanization dynamics. These approaches utilize the spatial and temporal information captured by remote sensing data to detect and analyze urban land cover changes. [6] Li, X., Liu, X., & Zhang, Y. (2014) conducted a study on urban expansion in Beijing, China, using remote sensing and spatial metrics. The authors analyzed Landsat images to identify land cover changes and applied spatial metrics to assess urban sprawl patterns and fragmentation.
Change Detection Algorithms: Various change detection algorithms have been developed to automatically identify and quantify urbanization changes from remote sensing data. These algorithms compare multi-temporal satellite images and highlight areas of significant land cover changes. Some commonly used change detection methods include:
Image differencing: This method involves subtracting corresponding pixel values of two or more images to identify areas of change. It is widely used for detecting urban growth and land cover changes.
Object-based change detection: Instead of comparing individual pixels, this approach groups pixels into objects or segments and evaluates changes at the object level. It considers both spectral and spatial characteristics, providing more accurate and detailed change detection results. Classification-based change detection: This method involves classifying multi-temporal images separately and then comparing the classified results to identify changes. It uses machine learning algorithms, such as Support Vector Machines (SVM) or Random Forest, to classify the images.

Spatial Analysis and Modeling: In addition to change detection, spatial analysis and modeling techniques play a crucial role in understanding and predicting urbanization patterns. These methods help assess the spatial distribution of urban growth, analyze urban expansion trends, and simulate future scenarios. Some relevant studies in this area includes [11] Seto, K. C., et al. (2011) employed a spatial econometric model to analyze the factors driving urban expansion in the Pearl River Delta, China. The study integrated remote sensing data, socio-economic variables, and spatial analysis techniques to identify the drivers of urbanization and predict future growth patterns. [23] Yuan, F., et al. (2005) developed a cellular automata model to simulate urban growth in Indianapolis, USA. The model incorporated spatial transition rules based on historical land cover changes and was used to forecast future urbanization scenarios. [26] Pontius, R. G., & Schneider, L. C. (2001) proposed the Geographical Information System-based Fuzzy Set (GIS-FS) approach for land change modeling.

This approach combines fuzzy set theory and GIS techniques to model land cover changes and urbanization processes.

Integration of Social and Environmental Factors: Recognizing the complex interactions between urbanization and socio-environmental factors, several studies have emphasized the importance of integrating social and environmental data in spatio-temporal change detection of urbanization. These studies aim to capture the socio-economic drivers' environmental impacts of urbanization and provide a more comprehensive understanding of the process. Some notable studies focusing on the integration of social and environmental factors in spatio-temporal change detection of urbanization include: [24] Ge, Y., et al. (2018) integrated remote sensing data, social media data, and socio-economic indicators to analyze urban growth patterns and their associated factors in the Yangtze River Delta, China. The study utilized a data fusion approach to incorporate social media data, such as geotagged photos and tweets, to capture human activities and preferences related to urbanization. [42] Lu, D., et al. (2004) combined remote sensing data with socio-economic data to analyze urban expansion and its environmental implications in the Phoenix metropolitan area, USA. The study integrated Landsat imagery, census data, and land use/land cover data to assess the relationship between urban growth and environmental factors, such as vegetation loss and land fragmentation.
[7] He, C., et al. (2019) investigated the spatio-temporal dynamics of urbanization and their impacts on urban heat islands in the Beijing-Tianjin-Hebei region, China. The study integrated satellite imagery, meteorological data, and socio-economic data to analyze the relationship between urbanization, land surface temperature, and socio-economic factors.

Chapter 4

4. Dataset Description

4.1. Remote Sensing

Remote sensing is a scientific method that involves acquiring information about the Earth's surface and atmosphere from a distance using sensors or instruments aboard aircraft or satellites. It is based on the principles of how objects interact with electromagnetic radiation.
Remote sensing encompasses the retrieval of Earth's parameters through the analysis of electromagnetic radiation measurements captured by sensors. It entails the detection and measurement of electromagnetic energy emitted or reflected by various materials in distant objects. a scientific method is used to gather information about the Earth's surface and atmosphere from a distance, which utilizes a range of techniques and sensors to detect and measure electromagnetic radiation. By employing electromagnetic sensors, remote sensing instruments capture data in different spectral bands, including visible, infrared, and microwave wavelengths. These sensors are designed to detect specific ranges of electromagnetic radiation and provide valuable insights into various aspects of the Earth's surface and atmosphere. This data is acquired in the form of digital images, where each pixel represents the radiation intensity for a specific location on the Earth's surface.

Remote sensing data is processed to enhance its quality and correct distortions, and it can be analyzed through techniques like image classification and data integration with GIS. Remote sensing finds applications in various fields, including environmental monitoring, agriculture and forestry, disaster management, urban planning, and Earth science. It is widely utilized in civil engineering for a variety of purposes, such as investigating watershed characteristics, simulating hydrological conditions and fluxes, constructing hydrological models, and providing crucial services for disaster management, including flood and drought monitoring and early warning systems.

Remote sensing can be categorized into two types based on the utilization of electromagnetic energy:

i) Passive Remote Sensing: In passive remote sensing, the energy source is naturally available, such as the sun. This mode of remote sensing commonly employs solar energy as the source of electromagnetic radiation. It captures the reflected solar energy from objects using static or dynamic platforms, utilizing bands that are minimally affected by atmospheric interference. An example of passive remote sensing is capturing images with a camera in natural light.

ii) Active Remote Sensing: Active remote sensing involves a source that generates and emits electromagnetic radiation directly towards the target. The sensors on remote sensing platforms capture the energy reflected from the target. Microwave remote sensing is a specific form of active remote sensing. An example of active remote sensing is capturing images with a camera using a built-in flash.

Advantages of Remote Sensing:

- Remote sensing enables wide-area coverage and data collection, providing a comprehensive view of landscapes and environments.
- It allows for non-intrusive data collection, reducing the need for physical presence and minimizing the associated costs and risks.
- Remote sensing facilitates the monitoring and assessment of inaccessible or hazardous areas, expanding our understanding of remote regions.
- It enables the detection of subtle changes over time, aiding in the analysis of long-term trends and supporting informed decision-making.

4.2. Satellite Data

Satellite data refers to the valuable information acquired through sensors and instruments installed on orbiting satellites. It provides significant insights into diverse aspects of the Earth's surface, atmosphere, and space environment.

Satellite data acquisition involves sensing and measuring different forms of energy, such as visible and infrared light, microwaves, and radio waves. These satellites are equipped with sensors designed to detect specific wavelengths of electromagnetic radiation. Satellite data can be classified into various types based on the portion of the electromagnetic spectrum they capture. Optical data, obtained through optical sensors, records reflected sunlight across different spectral bands for tasks like land cover mapping and vegetation health monitoring. Radar data, acquired using radar sensors, emits and captures microwave signals for purposes such as topographic mapping and forest cover detection. Thermal data, collected by thermal sensors, measures emitted radiation within the thermal infrared region for analyzing temperature patterns and urban heat islands. Multispectral/hyperspectral data provides detailed information about material composition, finding applications in mineral exploration and environmental monitoring. LiDAR data, obtained through laser pulses, aids in generating elevation models and mapping vegetation structure. Satellite data varies in spatial and temporal resolution, with higher resolution offering more detailed information but covering smaller areas. Data access is typically provided by government agencies and commercial providers. Preprocessing of satellite data is often required to correct distortions, and specialized software packages facilitate processing, enhancement, classification, and spatial analysis. Satellite data finds applications in environmental monitoring, natural resource management, weather forecasting, urban planning, and emergency response.

Satellite data plays a pivotal role in scientific research, environmental monitoring, resource management, and decision-making processes. Its availability and accessibility have revolutionized our comprehension of the Earth's dynamics, providing invaluable insights into various phenomena occurring on our planet.

4.3. Landsat 8/9

Landsat 8/9, also referred to as the Landsat Data Continuity Mission (LDCM), is a collaborative endeavor between the United States Geological Survey (USGS) and NASA. It represents the latest addition to the esteemed Landsat program, renowned for its extensive collection of Earth observation data since its inception in 1972. Sensor Configuration: Landsat 8 features two primary sensors, namely the Operational Land Imager (OLI) and the Thermal Infrared Sensor (TIRS). These advanced sensors are responsible for capturing data across various spectral bands within the electromagnetic spectrum. Spectral Bands: Landsat 8 excels at capturing imagery across an impressive spectrum of 11 distinct bands. These bands cover visible, near-infrared, shortwave infrared, and thermal infrared regions, enabling precise analysis of land cover, vegetation health, water resources, and other significant Earth surface features.Spatial Resolution: The spatial resolution of Landsat 8 imagery exhibits variability across different bands. The OLI sensor offers a ground sampling distance (GSD) of 30 meters for most bands, while the panchromatic band boasts an enhanced resolution of 15 meters. Additionally, the TIRS sensor ensures a GSD of 100 meters.

Coverage: With its wide swath width spanning an impressive 185 kilometers, Landsat 8 ensures extensive coverage during each orbit. It operates in a near-polar orbit, facilitating global coverage within a 16-day repetitive cycle. Data Acquisition: Landsat 8's data acquisition process occurs continuously as it orbits the Earth. It proficiently captures imagery during both daylight and nighttime operations, thereby supporting a wide range of applications and research endeavors.Data Products: Following meticulous processing, the data collected by Landsat 8 is disseminated as Level-1 Data Products courtesy of the USGS. These products comprise meticulously calibrated and geometrically corrected imagery, conveniently available in an array of file formats, including GeoTIFF.

Applications: The versatility of Landsat 8/9 data manifests in various applications, encompassing but not limited to, some applications of Landsat 8/9 are:

- Monitoring land use changes and urban expansion.
- Assessing vegetation health and monitoring crop conditions.
- Mapping and monitoring water resources and aquatic ecosystems.
- Studying natural hazards such as wildfires, droughts, and floods.
- Supporting climate change research and monitoring environmental impacts.

4.3.1. Bands in Landsat 8/9

Here is a chart showing the bands of Landsat 8/9 and their corresponding wavelengths:

Band Number	Band Name	Wavelength Range (micrometers)
Band 1	Coastal/Aerosol	0.43 - 0.45
Band 2	Blue	0.45 - 0.51
Band 3	Green	0.53 - 0.59
Band 4	Red	0.64 - 0.67
Band 5	Near-Infrared (NIR)	0.85 - 0.88
Band 6	Short-Wave Infrared (SWIR) 1	1.57 - 1.65
Band 7	Short-Wave Infrared (SWIR) 2	2.11 - 2.29
Band 8	Panchromatic	0.50 - 0.68
Band 9	Cirrus	1.36 - 1.38
Band 10	Thermal Infrared (TIRS) 1	10.60 - 11.19
Band 11	Thermal Infrared (TIRS) 2	11.50 - 12.51

Note: The wavelength ranges provided are approximate and may vary slightly.

These bands capture different portions of the electromagnetic spectrum and are used for various purposes in remote sensing applications. The spectral information provided by these bands enables the analysis of land cover, vegetation health, water resources, and other Earth surface features.

4.4. VIIRS

VIIRS, the Visible Infrared Imaging Radiometer Suite, is an advanced sensor suite integrated into the Suomi National Polar-orbiting Partnership (Suomi NPP) satellite, jointly developed and launched by NASA and the National Oceanic and Atmospheric Administration (NOAA) in 2011.
Its primary objective is to deliver comprehensive global observations of the Earth's atmosphere, land surfaces, and oceans, contributing to various fields of scientific research and analysis.: VIIRS represents a state-of-the-art multi-spectral sensor system, proficiently capturing radiometric data across multiple spectral bands spanning the entire electromagnetic spectrum. This extensive coverage encompasses visible, near-infrared, and thermal infrared wavelengths, enabling precise measurement and analysis of Earth's radiative properties.

VIIRS excels in capturing imagery across an impressive 22 spectral bands, encompassing wavelengths from visible light to longwave infrared. These bands incorporate the visible, near-infrared, shortwave infrared. A distinctive feature of VIIRS lies in its remarkable Day-Night Band (DNB), designed to capture exceptionally low-light and nighttime observations. This extraordinary capability enables the detection and monitoring of city lights, auroras, fires, and other intriguing low-light phenomena, providing invaluable insights into urbanization, light pollution, and natural events occurring during the night.

Applications: VIIRS data finds diverse applications across numerous domains, including:

- Weather and Climate Monitoring: VIIRS data contributes significantly to weather forecasting, severe weather event tracking, and climate studies. It enables monitoring of cloud cover, aerosols, sea surface temperature, and atmospheric conditions, facilitating accurate predictions and in-depth analyses.

- Environmental Monitoring: VIIRS plays a vital role in monitoring land cover changes, vegetation health, ocean color, and water quality. It aids in the study of wildfires, coastal zone monitoring, and environmental impact assessment, supporting sustainable management and conservation efforts.

- Disaster Response: VIIRS data proves invaluable in disaster response efforts, providing critical information on the extent of wildfires, floods, and other natural disasters. It assists in damage assessment, search and rescue operations, and post-disaster recovery planning, improving overall disaster management capabilities.

4.4.1. Day Night Band (DNB)

The "Day Night Band" (DNB) is a specific sensor band used in satellite imagery technology, particularly in the field of Earth observation. The Day Night Band is part of the Visible Infrared Imaging Radiometer Suite (VIIRS) instrument, which is flown aboard the Suomi National Polar-orbiting Partnership (Suomi NPP) satellite and the NOAA-20 satellite.

The Day Night Band is unique because it can capture both daytime and nighttime images. It is sensitive to low light levels and can detect natural and man-made sources of light, such as city lights, wildfires, gas flares, and even the faint glow of airglow in the atmosphere. By observing Earth's surface at night, the Day Night Band helps monitor nocturnal weather phenomena, urban development, light pollution, and other nighttime activities. The imagery captured by the Day Night Band has various applications, including environmental monitoring, disaster response, urban planning, and studying human activity patterns. It provides valuable insights into the dynamic nature of Earth's surface during both daylight and nighttime hours.

4.5. Data Collection

For this study, a range of data sources was collected, including vector and raster data, satellite imagery, and other relevant datasets. These data were crucial for investigating the changes occurring in the specific area under study from 2017 to 2023. The satellite images were obtained from the United States Geological Survey (USGS) archives. The Landsat 7 satellite with Enhanced Thematic Mapper Plus (ETM+) provided eight spectral bands, while Landsat 8, equipped with the Operational Land Imager (OLI) and the Thermal Infrared Sensor (TIRS), offered a total of 11 bands, including panchromatic, ultra blue, and thermal infrared bands. These satellite images served as the primary data source for the analysis. Due to the rugged topography and limited local resources, this study relied predominantly on secondary databases and existing data sources. The inclusion of lakes in the analysis was constrained by the availability of sufficient resources for data collection and analysis. Overall, the data collection process encompassed the acquisition of relevant vector and raster data, satellite imagery from Landsat 7 and Landsat 8, and other pertinent datasets from reliable sources. These data formed the foundation for conducting the spatio-temporal analysis of the study area.

4.6. Image Classification

The processing of satellite images involves mapping and analyzing the information contained within the images. One important aspect of image analysis is classification, which is a technique in Geographic Information Systems (GIS) used for comparative analysis and detecting changes in various types of land uses over a specific period of time. There are three main techniques of image classification: supervised, unsupervised, and object-based classification. In the context of high-resolution data analysis, object-based classification is often preferred. Object-based classification involves considering the characteristics and spatial relationships of image objects rather than individual pixels, resulting in more accurate and meaningful classification results.

In the current study, the satellite images have been classified using supervised classification. Supervised classification involves providing training samples to the classification algorithm, where the analyst identifies representative areas of different land use types. These training samples guide the algorithm in determining the spectral signatures associated with each land use class. By using supervised classification, the study aims to detect and analyze the changes in land use from 2013 to 2023. Overall, image classification is a valuable technique in GIS analysis, allowing for the identification and monitoring of land use changes over time. Supervised classification, specifically utilized in this study, provides a systematic approach to detect and analyze the changes occurring in the study area.

4.6.1. Steps to download DNB Nightlight image

1. Open the Google Earth Engine website: Go to the Google Earth Engine website (https://earthengine.google.com/) and sign in with your Google account.
2. Open the Earth Engine Code Editor: Once you're signed in, click on the "Code Editor" tab at the top of the page. This will open the Earth Engine Code Editor interface.

3. Search for the nightlight dataset: In the Code Editor, click on the "Assets" tab on the left-hand side. Use the search bar to find the nightlight dataset you want to download. Google Earth Engine provides various datasets, including nightlight imagery from different sources and years. You can search for datasets like "DMSP-OLS Nighttime Lights" or "VIIRS Nighttime Day/Night Band" Example: 'NOAA/VIIRS/DNB/MONTHLY_V1/VCMCFG'.
4. Import the nightlight dataset: Once you've found the desired dataset, import it into your Earth Engine script by using the **ee.ImageCollection** or **ee.Image** function.Replace **'dataset_name'** with the actual name of the dataset you found.
5. Filter and select the specific image: Nightlight datasets often contain multiple images for different time periods. You can filter and select a specific image based on your requirements. For example, if you want to download the nightlight image for a specific year, you can use the **filterDate** function to filter the Image Collection by date and then select the first image using the **first** function, replace **'start_date'** and **'end_date'** with the desired date range for the image.
6. Define the region of interest: Specify the region for which you want to download the nightlight image. You can define a region using coordinates, a geometry object, or a feature.
7. Replace **x_min**, **y_min**, **x_max**, and **y_max** with the minimum and maximum values of the latitude and longitude coordinates that define the rectangular region.
8. Clip the image to the region of interest: Clip the nightlight image to the defined region of interest using the **clip** function. This will ensure that the downloaded image only contains data within the specified region.
9. Download the image: Finally, use the **Export.image.toDrive** function to export the clipped image to your Google Drive account. Specify the image, a name for the exported file, and the desired export parameters such as the file format (e.g., TIFF) and scale. Replace **'nightlight_image'** with the desired description for the exported file, **'export_folder'** with the name of the folder in your Google Drive where the image should be saved and adjust the **scale** parameter based on the desired resolution of the image.
10. Run the export: Click on the "Run" button in the Code Editor

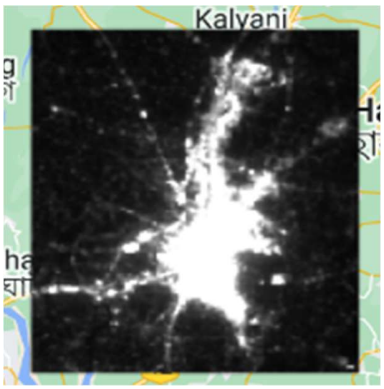

2012

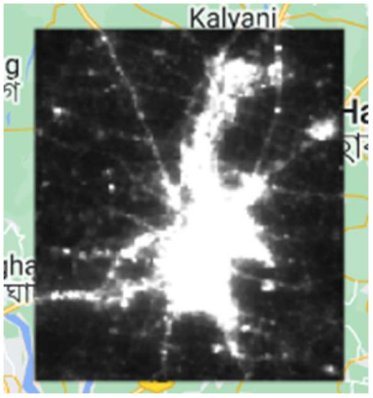

2022

4.6.2. Steps to download Landsat 8/9 dataset:

1. Visit the USGS EarthExplorer website: https://earthexplorer.usgs.gov/ using a web browser.

2. Click "Register" to create a new account or "Login" to access an existing account. Follow the provided instructions.
3. Once signed in, we will get reach the EarthExplorer main page.
4. Define your search criteria for finding Landsat imagery, including location, date range, sensor type, and data format.
5. In the "Search Criteria" tab, under "Data Sets," click "Additional Criteria" to choose the desired Landsat satellite for image downloads: Landsat 8 (OLI/TIRS) or Landsat 9 (TIRS-2/OLI-2).
6. Specify the spatial extent in the "Location" section of the "Search Criteria" tab. Enter an address, coordinates, draw a polygon, or use the provided tools to select an area of interest (AOI).
7. Also, indicate the desired date range for Landsat imagery.
8. Optionally, refine the search criteria by adjusting parameters like cloud cover and data collection level in the "Search Criteria" tab.
9. Initiate the search process by clicking the "Results" button at the bottom of the page.
10. Once the search is complete, thumbnail previews of available Landsat images will be displayed.
11. Review and select the desired images by checking the checkboxes next to them.
12. Add the selected images to your cart by clicking "Add to Cart."
13. Access the cart by clicking the "Cart" icon or navigating to the "Cart" tab.
14. Customize download options such as file format, projection, and other parameters.
15. Start the download process by clicking "Download" in the cart.
16. The chosen Landsat images will be downloaded to your computer in the specified format.
17. Allow sufficient time for the download to complete, considering the size and number of selected images.
18. Once the download is finished, locate the downloaded Landsat images on your computer.
19. Now we can then utilize these images for GIS analysis or visualization purposes.

4.6.3. Using Subsets via ROI on merged TIF image using Envi 4.7

1. Launch ENVI 4.7: Open the ENVI 4.7 software on your computer.
2. Open the merged TIF image: Go to "File"> "Open Image File" or use the shortcut Ctrl+O to import the merged TIF image into ENVI. Locate and select the merged TIF image file from your computer's file system, and click "OK" to open it.
3. Display the merged image: Once the image is open, it will be displayed in the ENVI viewer. You can explore the image and adjust the display settings such as brightness, contrast, and color stretch as needed.
4. Define the ROI: In the ENVI viewer, click on the "ROI" menu at the top and select "Define ROI" from the dropdown menu. This will activate the ROI Tools dialog.

5. Choose the ROI shape: In the ROI Tools dialog, select the desired shape for your ROI, such as rectangle, circle, polygon, or point. Choose the shape that best suits your analysis needs.

6. Draw the ROI on the merged image: Use your mouse to draw the ROI shape on the merged image in the ENVI viewer. For example, if you chose the rectangle shape, click and drag the mouse to create a rectangle around the area of interest. Ensure that the ROI encompasses the desired subset area.

7. Adjust the ROI properties (optional): After drawing the ROI, you can adjust its properties in the ROI Tools dialog. For instance, you can modify the color, line width, and transparency of the ROI outline by clicking on the "ROI Options" button in the dialog.

8. Apply the ROI subset: Once the ROI is defined and adjusted, go to the "ROI" menu again and select "Apply ROI as Subset" from the dropdown menu. This action will create a subset of the merged image based on the defined ROI.

9. Save the ROI subset: To save the ROI subset as a separate image file, go to "File" > "Save As" or use the shortcut Ctrl+Shift+S. Choose the desired file format (e.g., TIF) and provide a name and location for the subset file. Click "Save" to save the subset image.

10. Access and use the ROI subset: The saved ROI subset will be available for further analysis and processing in ENVI. You can open the subset image in ENVI, apply additional enhancements or algorithms, and use it in various geospatial workflows or export it to other software for further analysis.

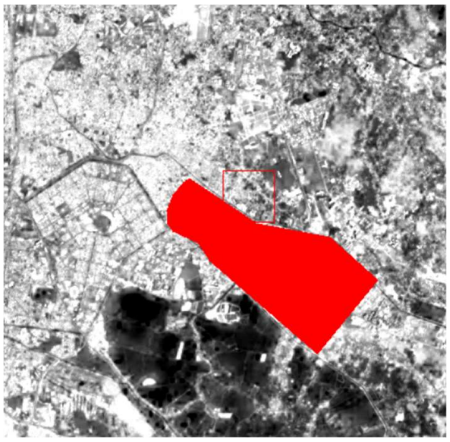

ROI 2023

Chapter 5

5. Methodology

A project management methodology is a kind of system comprising of several principles, techniques and procedures which are used by those who work in a disciplined manner. It acts as a body of methods, rules a postulate employed by a discipline. Project management methodologies are the essential different ways so that we can approach a project.

5.1. Flowchart

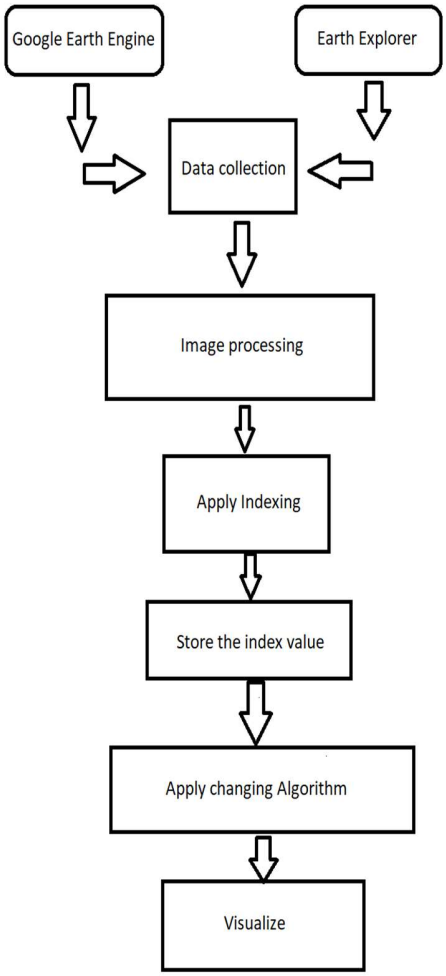

The Google Earth Engine is a geospatial processing service. With Earth Engine we can perform geospatial processing within a scale, and hence powered by Google Cloud Platform. Then we enter earth explorer and all the data regarding our study is collected. The data or the images collected are then processed or we can say we perform image processing. After that we apply indexing on the required data. Changing Algorithm is then applied on the applying index. Lastly, we can visualize the required changes and our work is done.

5.2. Normalized Difference Vegetation Index (NDVI):

NDVI (Normalized Difference Vegetation Index) is a commonly used vegetation index in remote sensing to assess vegetation health and vigor. It quantifies the amount of live green vegetation present in satellite imagery. The formula for calculating NDVI is as follows:

$$NDVI = (NIR - Red) / (NIR + Red)$$

Where:

- NIR refers to the reflectance value in the near-infrared spectral band.
- Red refers to the reflectance value in the red spectral band.

or Landsat imagery, the near-infrared (NIR) band corresponds to Landsat band 5 (0.85 - 0.88 micrometers), and the red band corresponds to Landsat band 4 (0.64 - 0.67 micrometers). The resulting NDVI values range from -1 to +1. Higher positive values indicate healthier and more abundant vegetation, while lower or negative values indicate less vegetation or non-vegetated areas (such as water or barren land). NDVI is widely used to monitor vegetation growth, assess vegetation stress, identify land cover types, and study changes in vegetation over time. It provides valuable information for agricultural monitoring, forestry management, and ecological studies about the frequency of occurrence of different values within a specified range. The length of a histogram depends on the number of bins used to divide the range of values.

5.3. Normalized Difference Built-up Index (NDBI):

NDBI (Normalized Difference Built-up Index) is a commonly used index in remote sensing to detect built-up areas in satellite imagery. It quantifies the degree of urbanization or the presence of built-up surfaces within an image pixel. The formula for calculating NDBI is as follows:

$$NDBI = (SWIR2 - NIR) / (SWIR2 + NIR)$$

Where:

- SWIR2 refers to the reflectance value in the Short-Wave Infrared (SWIR) band 2.
- NIR refers to the reflectance value in the Near-Infrared (NIR) band.

The SWIR2 band typically corresponds to Landsat band 7 (2.11 - 2.29 micrometers), and the NIR band corresponds to Landsat band 5 (0.85 - 0.88 micrometers). The resulting NDBI values range from -1 to +1. Positive values indicate the presence of built-up areas, while negative values represent non-built-up or natural surfaces. A threshold can be applied to classify pixels as built-up or non-built-up based on the NDBI values. It's important to note that the specific band combinations and thresholds for NDBI may vary depending on the sensor or dataset being used. Additionally, atmospheric correction and image preprocessing may be necessary before calculating the NDBI to ensure accurate results.

5.4. Normalized Difference Water Index (NDWI):

NDWI (Normalized Difference Water Index) is another widely used index in remote sensing to identify water bodies within satellite imagery. It is particularly effective in distinguishing between water and land surfaces. The formula for calculating NDWI is as follows:

$$NDWI = (Green - NIR) / (Green + NIR)$$

Where:

- Green refers to the reflectance value in the green spectral band.
- NIR refers to the reflectance value in the near-infrared spectral band.

The Green band typically corresponds to Landsat band 3 (0.53 - 0.59 micrometers), and the NIR band corresponds to Landsat band 5 (0.85 - 0.88 micrometers). The resulting NDWI values range from -1 to +1. Higher positive values indicate the presence of water, while lower values represent land surfaces. A threshold can be applied to classify pixels as water or land based on the NDWI values.It's important to note that the specific band combinations and thresholds for NDWI may vary depending on the sensor or dataset being used. Additionally, atmospheric correction and image preprocessing may be necessary before calculating the NDWI to ensure accurate results.

5.5. Block Based and Cell Based Along with Histogram's Length

Block-based: In image or video processing, block-based methods refer to techniques where the image or video is divided into rectangular blocks of pixels. These blocks are then processed individually, often for tasks such as compression, motion estimation, or object recognition. By dividing the image into blocks, computations can be performed more efficiently, and spatial dependencies within each block can be exploited.

Cell-based: Cell-based methods are often used in computer vision, particularly in the field of object detection or image segmentation. Here, the image is divided into smaller cells or regions, typically of fixed size and shape, which are analyzed individually. These cells are often organized in a grid-like structure, such as a grid of squares or hexagons. Features or descriptors are computed for each cell, and these features are used to classify objects or segment the image.

Histogram length, on the other hand, refers to the number of bins or discrete values in a histogram. A histogram represents the distribution of pixel intensities or other features in an image. It provides information about the frequency of occurrence of different intensity values or features within the image. By analyzing the histogram, we can gain insights into the overall brightness, contrast, and distribution characteristics of the image, which can be useful for image enhancement, thresholding, and other image processing tasks.

5.5.1. Cell Based Weighted Difference for NDVI

The Cell-based Weighted Difference (CWD) is a widely used technique for analyzing remote sensing data, particularly the Normalized Difference Vegetation Index (NDVI). NDVI is a commonly used vegetation index that provides information about the health and density of vegetation cover. The CWD method calculates the difference between two NDVI images on a cell-by-cell basis, where each cell represents a specific location on the Earth's surface, typically corresponding to a pixel in the remote sensing imagery. This difference is then weighted by the values of a third image, which can represent various parameters related to vegetation, land cover, or other factors of interest.

5.5.2. Block Based Weighted Difference for NDVI

"Block-based Weighted Difference" is not a standardized term or technique, I can provide you with a generalized approach that combines block-based analysis and weighting for comparing NDVI values. Here's a potential method: Divide the NDVI images: Split both NDVI images into non-overlapping blocks or patches of equal size. The size of the blocks will depend on your specific analysis requirements, such as the spatial scale or the extent of the areas you want to compare.Calculate block-level NDVI: For each block in both NDVI images, calculate a representative NDVI value. This can be achieved by summarizing the NDVI values within each block, such as taking the average, maximum, minimum, or any other relevant statistic that represents the block's vegetation characteristics.

Prepare the weighting image: Determine a third image or layer that will serve as the weighting factor for the block-based comparison. Similar to the previous explanation, this image could represent land cover classification, vegetation density, or any other parameter relevant to your analysis. Assign weights to each block based on the values of this weighting image.Compute the weighted difference: Calculate the weighted difference between the block-level NDVI values of the two images. Multiply the difference between the NDVI values of the corresponding blocks by their respective weights obtained from the weighting image.

5.5.3. Cell Based and Block Based Weighted Difference for NDBI

Here's an explanation of both the Cell-based Weighted Difference and Block-based Weighted Difference for the Normalized Difference Built-up Index (NDBI):

Cell-based Weighted Difference for NDBI:

i. Obtain two NDBI images representing the time periods or conditions you want to compare.
ii. Prepare a third image as the weighting factor, which contains relevant information for your analysis.
iii. Ensure the images are spatially aligned and have the same resolution and reference system.5.5.
iv. Calculate the weighted difference for each corresponding cell: WD = Weight * (NDBI_2 - NDBI_1) where WD is the weighted difference, Weight is the value of the weighting image at that cell, NDBI_2 is the NDBI value from the second image, and NDBI_1 is the NDBI value from the first image.
v. Analyze the resulting weighted difference image to identify areas of significant change in NDBI, considering the weighting factors.

Block-based Weighted Difference for NDBI:

i. Divide both NDBI images into non-overlapping blocks or patches of equal size.
ii. Calculate a representative NDBI value for each block in both NDBI images.
iii. Prepare a weighting image that represents relevant information for the analysis.
iv. Compute the weighted difference between block-level NDBI values of the two images: WD = Weight * (NDBI_2 - NDBI_1) where WD is the weighted difference, Weight is the value of the weighting image for that block, NDBI_2 is the block-level NDBI value from the second image, and NDBI_1 is the block-level NDBI value from the first image.
v. Analyze the resulting weighted difference image to identify areas of significant change in NDBI, considering the weighting factors at the block level.

Both the cell-based and block-based approaches offer different ways to compare NDBI values, depending on the level of spatial detail and analysis objectives you have. The choice between these methods should consider the specific requirements of your analysis, such as the scale of built-up areas you want to analyze and the characteristics of the data available.

5.5.4. Cell-Based and Block-Based Weighted Difference for NDWI

The Cell-based Weighted Difference (CWD) and Block-based Weighted Difference (BWD) are two distinct approaches used to compare NDWI (Normalized Difference Water Index) values. These methods enable the analysis of changes in water content or presence over time or between different conditions.

Cell-based Weighted Difference for NDWI:

Obtain two NDWI images representing the desired time periods or conditions for comparison.Prepare a third image to serve as the weighting factor, containing relevant information related to the analysis, such as land cover types, water dynamics, or other factors influencing water distribution.Ensure that the images are spatially aligned, with the same resolution and reference system.

Calculate the weighted difference for each corresponding cell WD = Weight * (NDWI2 - NDWI1), where WD represents the weighted difference, Weight is the value of the weighting image at that cell, NDWI2 is the NDWI value from the second image, and NDWI1 is the NDWI value from the first image. Analyze the resulting weighted

difference image to identify areas of significant change in NDWI, taking into account the weighting factors applied.

Block-based Weighted Difference for NDWI:

Divide both NDWI images into non-overlapping blocks or patches of equal size.Calculate a representative NDWI value for each block in both NDWI images. This can be achieved by taking the mean, median, or other statistical measures of the NDWI values within each block.Prepare a weighting image that corresponds to the block-level analysis, containing information relevant to the study, such as water-related characteristics or land cover types. Compute the weighted difference between the block-level NDWI values of the two images: WD = Weight * (NDWI2 - NDWI1), where WD represents the weighted difference, Weight is the value of the weighting image for that block, NDWI2 is the block-level NDWI value from the second image, and NDWI1 is the block-level NDWI value from the first image. Analyze the resulting weighted difference image to identify areas of significant change in NDWI at the block level, considering the weighting factors applied. The choice between the cell-based and block-based approaches depends on the specific analysis objectives, spatial scale, and characteristics of the data. The cell-based method provides a fine-grained analysis by comparing NDWI values on a cell-by-cell basis, while the block-based method aggregates NDWI values within blocks, allowing for a broader analysis at a block level. Consider the spatial scale and resolution of the data when deciding which method is most suitable for your analysis.

5.6. Day Night Band (DNB)

The "Day Night Band" (DNB) is a specific sensor band used in satellite imagery technology, particularly in the field of Earth observation. The Day Night Band is part of the Visible Infrared Imaging Radiometer Suite (VIIRS) instrument, which is flown aboard the Suomi National Polar-orbiting Partnership (Suomi NPP) satellite and the NOAA-20 satellite.

The Day Night Band is unique because it can capture both daytime and nighttime images. It is sensitive to low light levels and can detect natural and man-made sources of light, such as city lights, wildfires, gas flares, and even the faint glow of airglow in the atmosphere. By observing Earth's surface at night, the Day Night Band helps monitor nocturnal weather phenomena, urban development, light pollution, and other nighttime activities. The imagery captured by the Day Night Band has various applications, including environmental monitoring, disaster response, urban planning, and studying human activity patterns. It provides valuable insights into the dynamic nature of Earth's surface during both daylight and nighttime hours.

5.6.1. Cell Based Weighted Difference for VIIRS DNB

The cell-based weighted difference of electricity is a measure that utilizes the Nighttime Lights dataset captured by the Day/Night Band (DNB) sensor. The Nighttime Lights dataset provides information on the brightness of lights observed during the nighttime, which can be used as a proxy for human activity and electricity consumption.
To calculate the cell-based weighted difference of electricity, the following steps are typically followed:

i) Obtain the Nighttime Lights dataset, specifically the band captured by the Day/Night Band (DNB) sensor. This dataset contains pixel values representing the brightness of lights observed during the nighttime.

ii) Define a study area or region of interest (ROI) where you want to analyze the electricity consumption patterns.

iii) Divide the study area into cells or grid cells of a specific size. The size of the cells can vary depending on the resolution of the Nighttime Lights dataset and the level of detail required for the analysis.

iv) For each cell, calculate the average or weighted average of the Nighttime Lights values within that cell. The weighting can be based on various factors such as population density, land use patterns, or other relevant socioeconomic indicators. This step aims to account for the varying contributions of different areas within a cell to the overall electricity consumption estimate.

v) Calculate the difference in the weighted average Nighttime Lights values between different time periods or regions of interest. This difference represents the cell-based weighted difference of electricity, indicating the change or variation in electricity consumption over time or across different areas.

vi) By analyzing the cell-based weighted difference of electricity, researchers and policymakers can gain insights into changes in electricity consumption patterns, identify areas of high or low electricity consumption, monitor trends, and assess the effectiveness of energy conservation measures or policies.

5.7. Threshold Strategy

The threshold strategy involves establishing a specific cutoff value to classify data or determine the course of action. It is widely used in fields such as remote sensing, data analysis, risk management, and quality control. The goal is to simplify complex data into discrete categories or identify critical points for decision-making. Clearly to identify the purpose of the analysis and the specific decision or outcome to be made based on the data. By determining the cutoff value that will classify the data or trigger a particular action. This is often based on scientific knowledge, expertise, or desired outcomes.The threshold strategy finds application in various contexts. For instance, in remote sensing, it is used to classify satellite imagery into land cover types or identify specific features like water bodies or vegetation. In risk management, thresholds can trigger actions based on predefined risk levels, while in quality control, thresholds determine if a product or process meets standards.

The selection of an appropriate threshold is critical and should be based on a careful analysis of the data, domain knowledge, and the desired outcomes. The threshold strategy provides a systematic and objective approach to decision-making and classification, allowing for efficient data analysis and informed decision-making.

5.7.1. OTSU'S Method

The Otsu method, also known as Otsu's thresholding, is a popular technique utilized for automatic image thresholding. Its purpose is to determine an optimal threshold value to separate an image into foreground and background regions based on grayscale intensity values.

The Otsu method involves the following steps:

I. Compute the histogram of the input image, which represents the distribution of pixel intensities.
II. Count: Determine the total number of pixels in the image.
III. Calculate the cumulative sum of the histogram, representing the cumulative probability of each grayscale intensity value.
IV. Calculate the cumulative mean value by dividing the cumulative sum by the total number of pixels. This step helps estimate the mean intensity values of the foreground and background regions.

The Otsu method is widely utilized due to its ability to automatically determine the threshold value based on the image's histogram, without requiring prior knowledge or manual intervention. It is particularly effective for images with bimodal intensity distributions, where distinct intensity peaks exist in the foreground and background regions. The method can be applied to grayscale images as well as individual channels of color images. By accurately separating the foreground and background regions, the Otsu method finds application in various image processing tasks, including image segmentation, object detection, and feature extraction. It enables efficient analysis and manipulation of images, contributing to advancements in computer vision and pattern recognition.

Chapter 6

6.1. Experimental Data Analysis

6.1.1. NDBI 2013 and 2023 difference

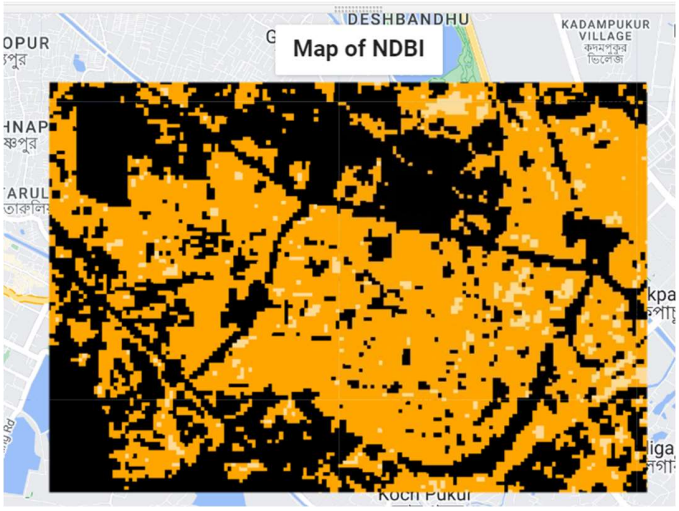

2013 NDBI

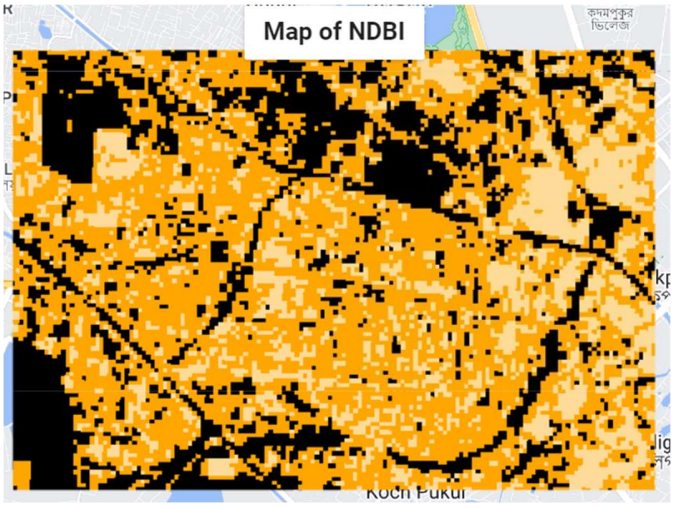

2023 NDBI

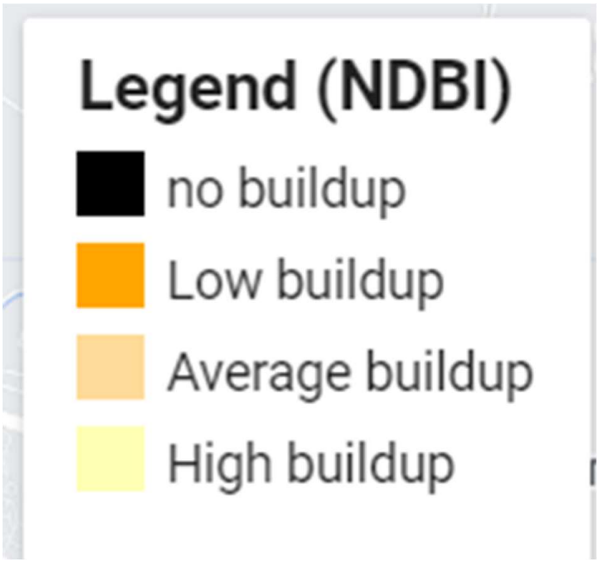

6.2.2. 2013 and 2023 NDWI Difference

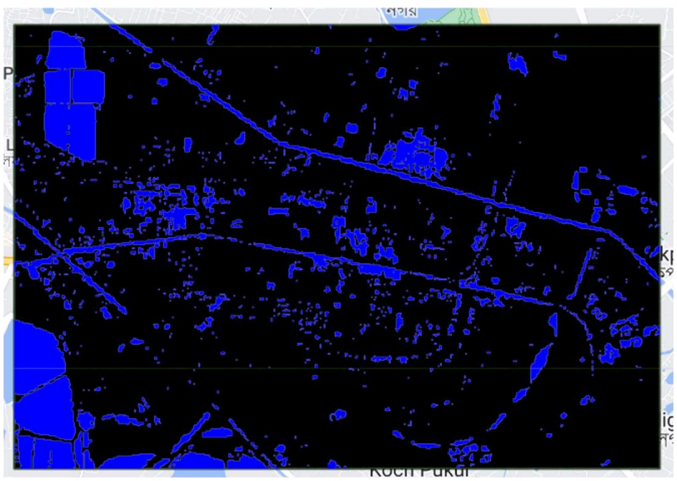

2013 NDWI

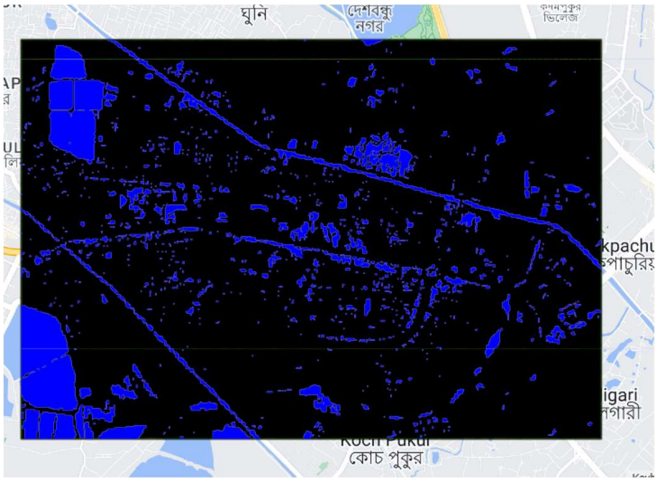

2023 NDWI

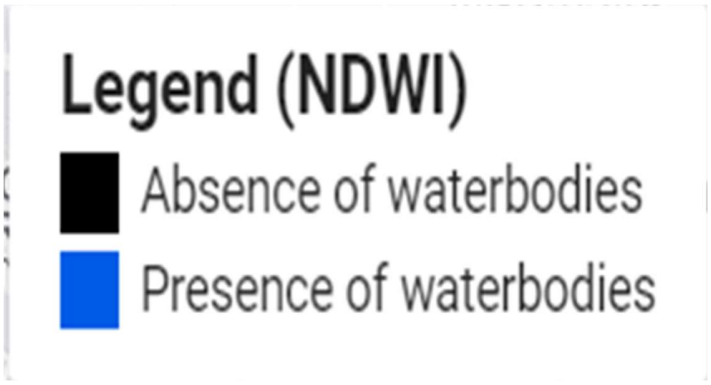

6.2.3. 2013 and 2023 NDVI Difference

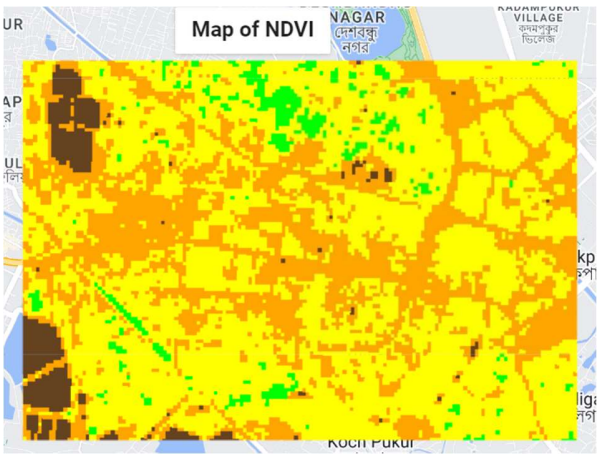

2013 NDVI

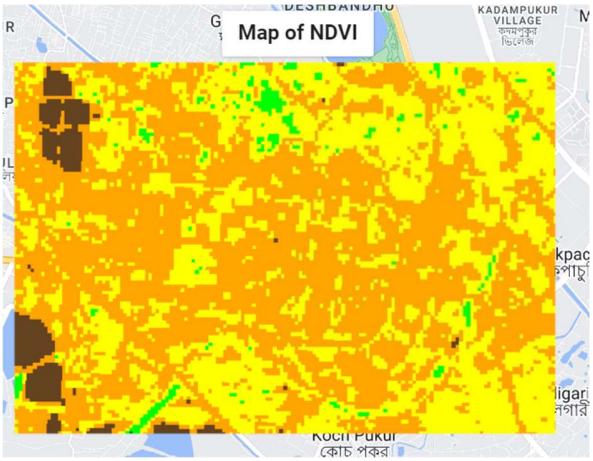

2023 NDVI

6.2.4. Day/Night Band (DNB)

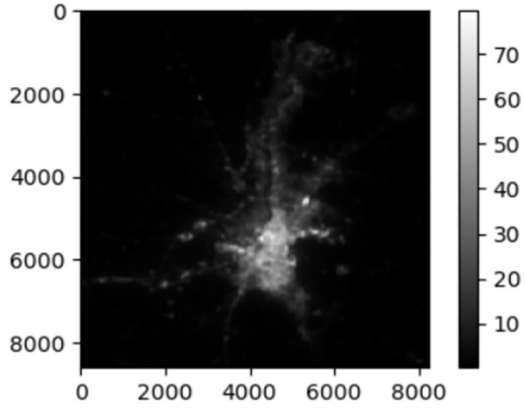

2012

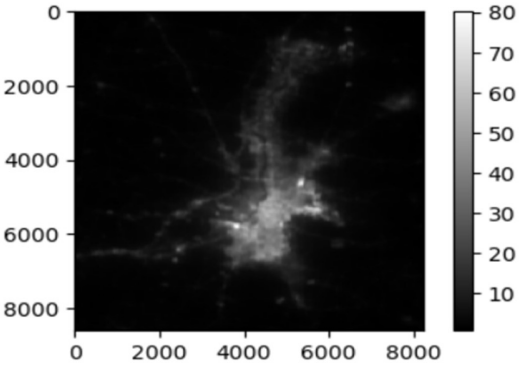

2022

6.2.5. Cell Based Weighted Distance Difference for NDVI

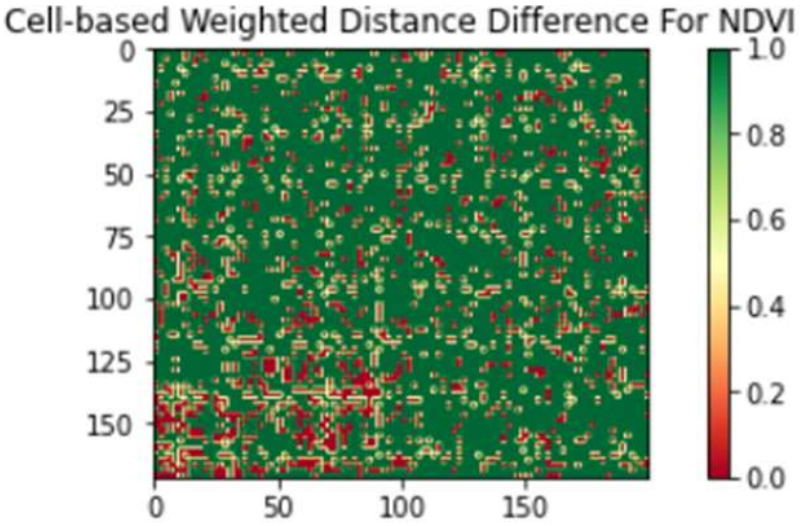

6.2.6. Block Based Weighted Distance Difference for NDVI

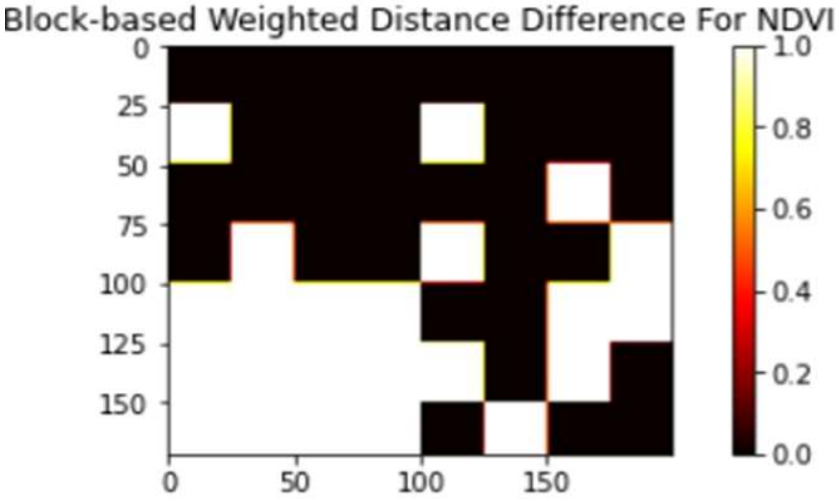

6.2.7. Cell and Block Based Weighted Distance Difference for NDBI

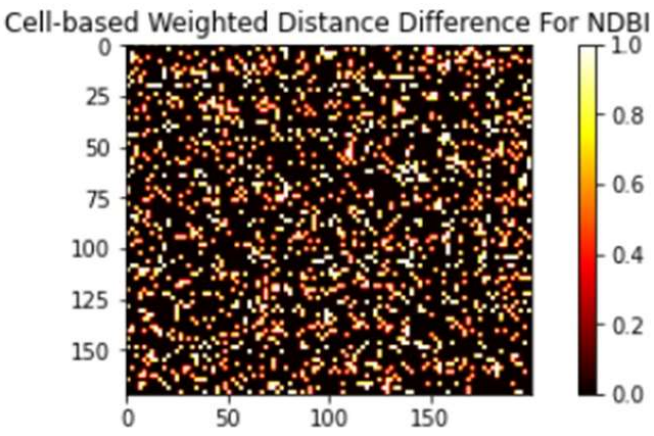

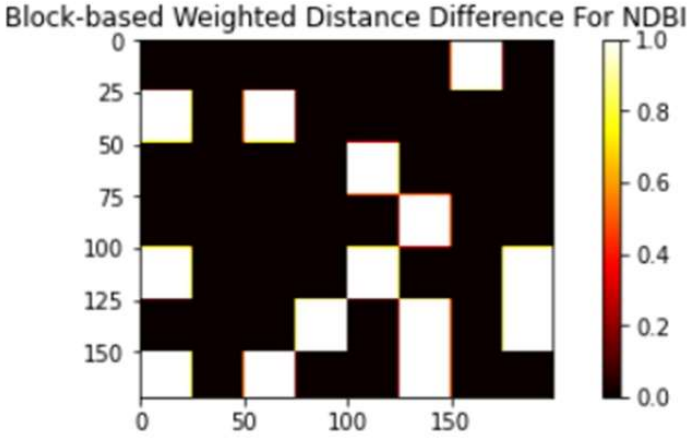

6.2.8. Cell and Block Based Weighted Distance Difference for NDWI

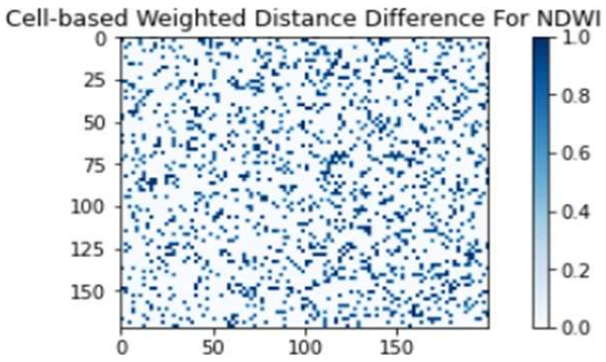

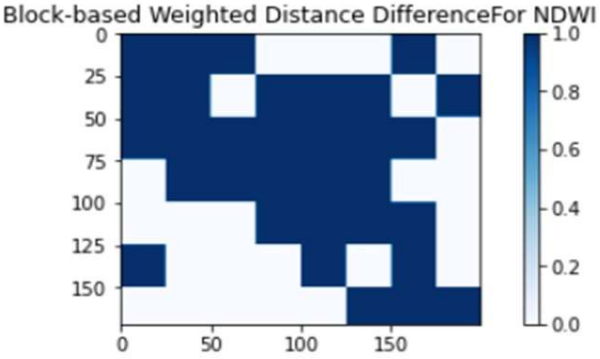

6.2.9. Cell Based Weighted Distance Difference for Electricity

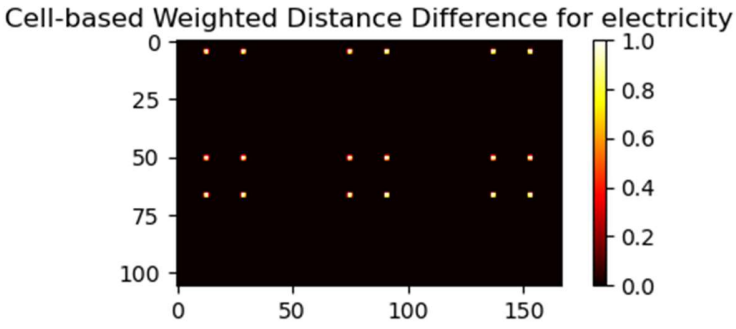

6.2.10. Cell Based Weighted Distance Difference Comparison

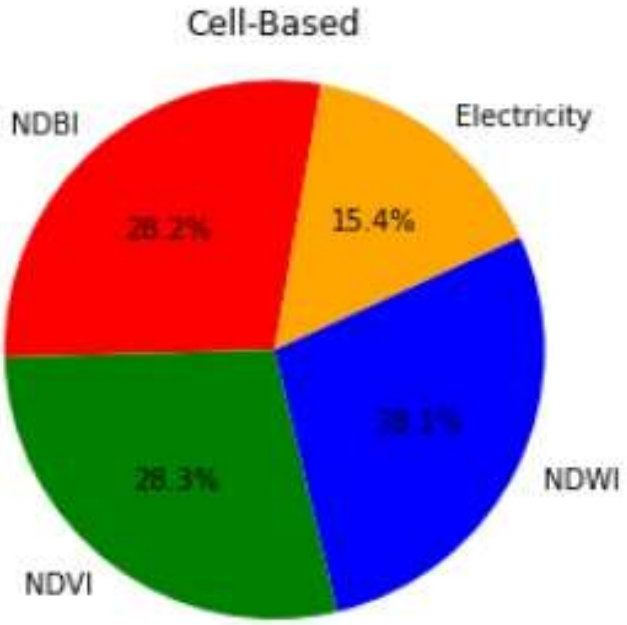

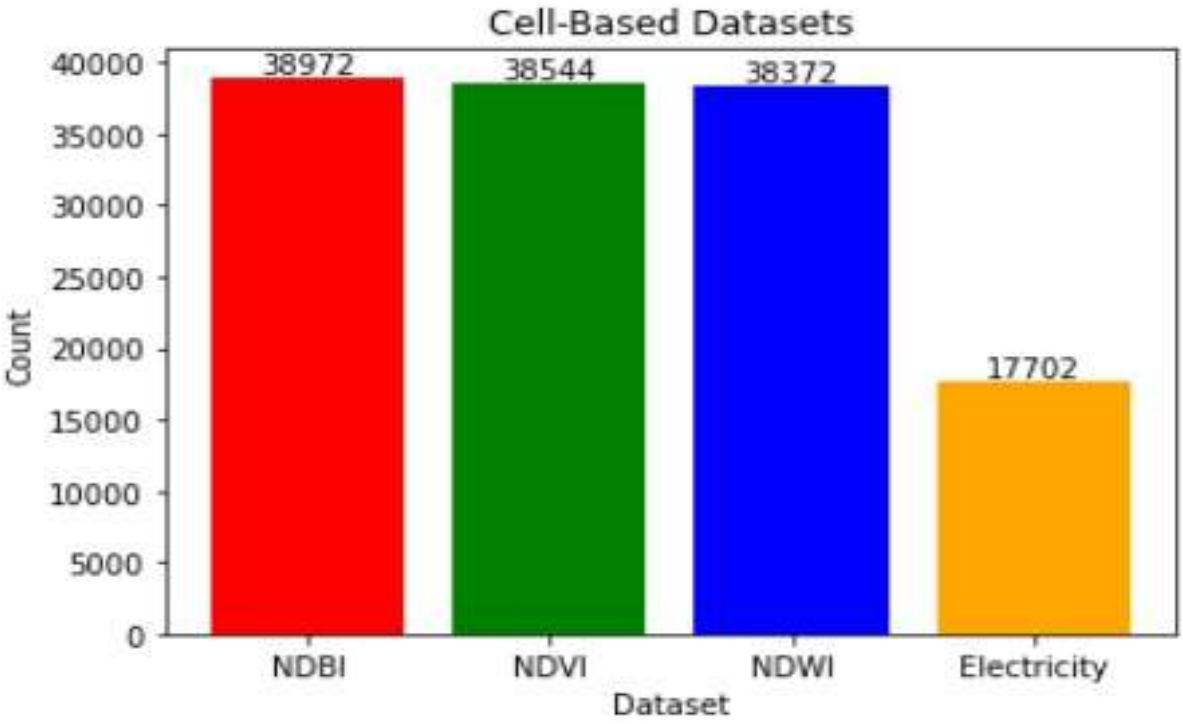

6.2.11. Block Based Weighted Distance Difference Comparison

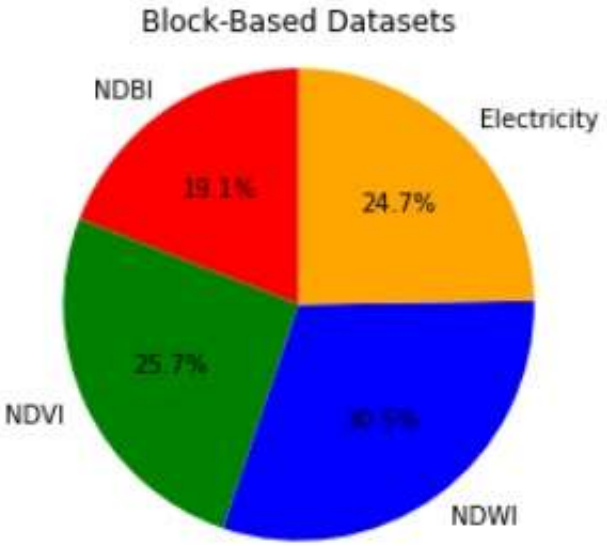

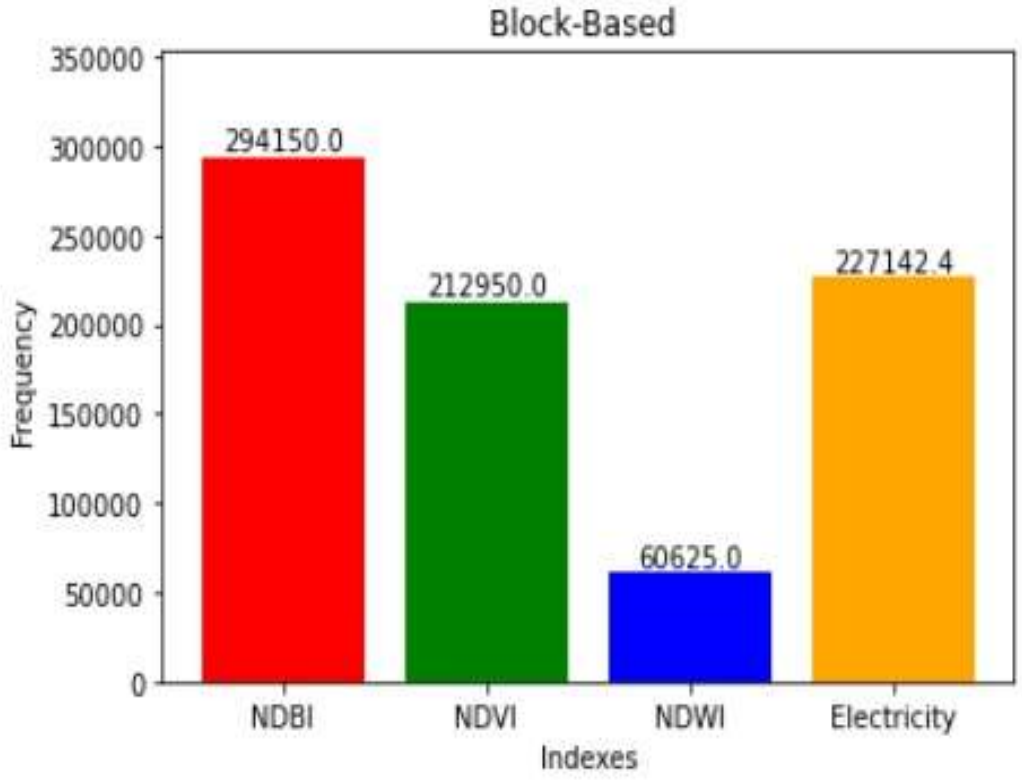

Conclusion

Spatio-temporal change detection of urbanization plays a crucial role in understanding urban dynamics, supporting decision-making processes, and promoting sustainable urban development. Remote sensing, GIS, and advanced analytical techniques offer valuable tools for monitoring and analyzing urbanization changes. However, challenges related to data availability, accuracy, scale, and contextual analysis need to be addressed to improve the effectiveness of change detection methods. Future research should focus on integrating multi-source data, exploring advanced machine learning algorithms, and developing standardized approaches for urban change detection and monitoring.

Future Scope

The future scope of a project on spatio-temporal change of urbanization using satellite data and indices like NDVI, NDWI, NDBI, and electricity index can include several avenues for further research and applications. Here are some potential future directions:

Long-term Monitoring: Extend the study to encompass a longer time period to capture more comprehensive trends and patterns of urbanization. Analyze the changes over multiple decades to understand the long-term dynamics of urban growth and its impact on the environment.

Fine-scale Analysis: Refine the spatial resolution of the satellite data or utilize higher-resolution imagery to analyze urbanization at a finer scale. This can provide more detailed insights into intra-urban variations, land-use changes, and their impacts on local ecosystems and communities.

Integration of Multi-source Data: Incorporate additional data sources such as socioeconomic data, transportation networks, or population demographics to examine the relationship between urbanization dynamics and social or economic factors. Integrating data from different domains can lead to a more holistic understanding of urbanization processes.

Machine Learning and AI Techniques: Explore the application of machine learning and artificial intelligence techniques to automate the analysis and detection of urbanization changes. Develop predictive models that can forecast future urbanization patterns based on historical data and other relevant variables

Collaboration with Stakeholders: Engage with local authorities, urban planners, environmental agencies, or non-governmental organizations to collaborate on applying the research outcomes to real-world scenarios. Seek partnerships to implement the findings in urban development projects, land-use planning, or environmental management initiatives.

Time-series Analysis: Analyze the historical satellite data and derived indices over a specific time period. Identify temporal patterns and trends in urbanization, such as the rate of growth, seasonal variations, or cyclic patterns.

Interpretation and Communication: Interpret and communicate the predictions, highlighting potential future urbanization trends, areas of high growth, or areas prone to specific changes.

REFERENCES

[1] R. R Navalgund and V.Tamilarasan, “Remote Sensing for Rural Development”, Journal of Rural Development, Vol. 17(3), pp. 421-441(1998), NIRD, Hyderabad

[2] Sumayyah Abdul Aziz, Ruzita Mohd Amin, Selamah Abdullah Yusof, Mohamed Aslam Haneef, Mustafa Omar Mohamed and Gapur Oziev, “A Critical Analysis of Development Indices”, Australian Journal of Sustainable Business and Society, Vol. 01 No. 01(March 2015)

[3] Sen, A. (1999), “Development as freedom”, Oxford: Oxford University Press.

[4] Mahbub ul Haq 1995, “Reflections on Human Development”, Oxford University Press, New York.

[5]A Comparative Study of Urban Expansion in Beijing, Tianjin and Tangshan from the 1970s to 2013

[6] Land Cover Changes and Urban Expansion in Chongqing, China: A Study Based on Remote Sensing Images, Li, X., Liu, X., & Zhang, Y. (2014)

[7] He, C., et al. (2019) Investigation of the spatio-temporal dynamics of urbanization and their impacts on urban heat islands in the Beijing-Tianjin-Hebei region, China.

[8] D Nagesh Kumar, IISc, Bangalore, “Remote Sensing: Introduction and Basic Concepts”, NPTEL

[9] Cem Unsalan, Kim L. Boyer, “Multispectral Satellite Image Understanding-From Land Classification to Building and Road Detection”, Chapter2 pp1-10, Springer-Verlag London.

[10] "Sentinel-2 MSI: Overview". European Space Agency. Retrieved 17 June 2015.

[11] Cole, T.A., Wanik, D.W., Molthan, A.L., Román, M.O., Griffin, R.E., 2017. “Synergistic use of night-time satellite data, electric utility infrastructure, and ambient population to improve power outage detections in urban areas.” Remote Sens. 9, 286. http://dx.doi.org/10.3390/rs9030286.

[12] Mann, M.L., Melaas, E.K., Malik, A., 2016. “Using VIIRS day/night band to measure electricity supply reliability: preliminary results from Maharashtra, India.” Remote Sens. 8, 711.

[13] Molthan, A., Jedlovec, G., 2013. “Satellite observations monitor outages from superstorm Sandy.” Eos. Trans. Am. Geophys. Union 94, 53–54.

[14] Polivka, T.N., Wang, J., Ellison, L.T., Hyer, E.J., Ichoku, C.M., 2016. “Improving nocturnal fire detection with the VIIRS day–night band.” IEEE Trans. Geosci. Remote Sens. 54,5503–5519.

[15] Asanuma, I., Yamaguchi, T., Park, J., Mackin, K.J., Mittleman, J., 2016. “Detection limit of fishing boats by the day night band (DNB) on VIIRS. In: SPIE Optical Engineering + Applications.” International Society for Optics and Photonics (p.99760P–99760P–8).

[16] Elvidge, C.D., Zhizhin, M., Baugh, K., Hsu, F.-C., 2015. “Automatic boat identification system for VIIRS low light imaging data.” Remote Sens. 7, 3020–3036.

[17] Straka, W.C., Seaman, C.J., Baugh, K., Cole, K., Stevens, E., Miller, S.D., 2015. “Utilization of the suomi national polar-orbiting partnership (npp) visible infrared imaging radiometer suite (viirs) day/night band for arctic ship tracking and fisheries management.” Remote Sens. 7, 971–989.

[18] Bankert, R.L., Solbrig, J.E., Lee, T.F., Miller, S.D., 2011. “Automated lightning flash detection in nighttime visible satellite data.” Weather Forecast. 26, 399–408.

[19] Hu, C., Chen, S., Wang, M., Murch, B., Taylor, J., 2015. “Detecting surface oil slicks using VIIRS nighttime imagery under moon glint: a case study in the Gulf of Mexico.” Remote Sens. Lett. 6, 295–301.

[20] Elvidge, C.D., Zhizhin, M., Baugh, K., Hsu, F.-C., Ghosh, T., 2015. “Methods for global survey of natural gas flaring from visible infrared imaging radiometer suite data.” Energies 9, 14.

[21] Liu, Y., Wang, Z., Sun, Q., Erb, A.M., Li, Z., Schaaf, C.B., Zhang, X., Román, M.O., Scott, R.L., Zhang, Q., 2017. “Evaluation of the VIIRS BRDF, Albedo and NBAR products suite and an assessment of continuity with the long-term MODIS record.” Remote Sens.Environ. 201, 256–274.

[22] Minnis, P., Hong, G., Sun-Mack, S., Smith, W.L., Chen, Y., Miller, S.D., 2016. “Estimating nocturnal opaque ice cloud optical depth from MODIS multispectral infrared radiances using a neural network method.” J. Geophys. Res. Atmos. 121, 4907–4932. http://dx.doi.org/10.1002/2015JD024456.

[23] Yuan, F., et al. (2005) Development of a cellular automata model to simulate urban growth in Indianapolis, USA.

[24] Ge, Y., et al. (2018) Integration of remote sensing data, social media data, and socio-economic indicators to analyze urban growth patterns in the Yangtze River Delta, China.

[25] McHardy, T.M., Zhang, J., Reid, J.S., Miller, S.D., Hyer, E.J., Kuehn, R.E., 2015. “An improved method for retrieving nighttime aerosol optical thickness from the VIIRS day/night band.” Atmos. Meas. Tech. 8, 4773–4783.

[26] Pontius, R. G., & Schneider, L. C. (2001) Proposal of the Geographical Information System-based Fuzzy Set (GIS-FS) approach for land change modeling.

[27] Miller, S.D., Straka, W.C., Yue, J., Smith, S.M., Alexander, M.J., Hoffmann, L., Setvák, M.,Partain, P.T., 2015. “Upper atmospheric gravity wave details revealed in nightglow satellite imagery.” Proc. Natl. Acad. Sci. 112, E6728–E6735.

[28] Bickenbach, F., Bode, E., Nunnenkamp, P., Söder, M., 2016. “Night lights and regional GDP.” Rev. World Econ. 152, 425–447. http://dx.doi.org/10.1007/s10290-016-0246-0.

[29] Chen, X., Nordhaus, W., 2015. A test of the new VIIRS lights data set: population and economic output in Africa. Remote Sens. 7, 4937–4947. http://dx.doi.org/10.3390/rs70404937.

[30] Huang, Q., Yang, X., Gao, B., Yang, Y., Zhao, Y., 2014. “Application of DMSP/OLS nighttime light images: a meta-analysis and a systematic literature review.” Remote Sens. 6, 6844–6866. http://dx.doi.org/10.3390/rs6086844.

[31] Wolfe, R.E., Lin, G., Nishihama, M., Tewari, K.P., Tilton, J.C., Isaacman, A.R., 2013. “Suomi NPP VIIRS prelaunch and on-orbit geometric calibration and characterization.” J. Geophys. Res. Atmos. 118.

[32] Lee, S., McIntire, J., Oudrari, H., Schwarting, T., Xiong, X., 2015. “A new method for Suomi-NPP VIIRS day–night band on-orbit radiometric calibration.” IEEE Trans. Geosci. Remote Sens. 53, 324–334. http://dx.doi.org/10.1109/TGRS.2014.2321835.

[33] Liao, L.B., Weiss, S., Mills, S., Hauss, B., 2013. “Suomi NPP VIIRS day-night band on-orbit performance.” J. Geophys. Res. Atmos. 118, 12705–12718. http://dx.doi.org/10.1002/2013JD020475.

[34] Xiong, X., Butler, J., Chiang, K., Efremova, B., Fulbright, J., Lei, N., McIntire, J., Oudrari, H., Sun, J., Wang, Z., 2014. “VIIRS on-orbit calibration methodology and performance.” J. Geophys. Res. Atmos. 119, 5065–5078.

[35] Zhang, Q., Pandey, B., Seto, K.C., 2016. “A robust method to generate a consistent time series from DMSP/OLS nighttime light data.” IEEE Trans. Geosci. Remote Sens. 54, 5821–5831.

[36] Campagnolo, M.L., Sun, Q., Liu, Y., Schaaf, C., Wang, Z., Román, M.O., 2016. “Estimating the effective spatial resolution of the operational BRDF, albedo, and nadir reflectance products from MODIS and VIIRS. Remote Sens. Environ.” 175, 52–64.

[37] Pahlevan, N., Sarkar, S., Devadiga, S., Wolfe, R.E., Román, M., Vermote, E., Lin, G., Xiong, X., 2017. “Impact of spatial sampling on continuity of MODIS–VIIRS land surface reflectance products: a simulation approach.” IEEE Trans. Geosci. Remote Sens. 55, 183–196.

[38] Miller, Mills, S.P., Elvidge, C.D., Lindsey, D.T., Lee, T.F., Hawkins, J.D., 2012a. “Suomi satellite brings to light a unique frontier of nighttime environmental sensing capabilities.” Proc. Natl. Acad. Sci. 109, 15706–15711. http://dx.doi.org/10.1073/pnas.1207034109.

Miller, S.D., Combs, C.L., Kidder, S.Q., Lee, T.F., 2012b. “Assessing moonlight availability for nighttime environmental applications by low-light visible polar-orbiting satellite sensors.” J. Atmos. Ocean. Technol. 29, 538–557. http://dx.doi.org/10.1175/JTECHD-11-00192.1.

[39] Miller, S.D., Turner, R.E., 2009. “A dynamic lunar spectral irradiance data set for NPOESS/VIIRS day/night band nighttime environmental applications.” IEEE Trans. Geosci.Remote Sens. 47, 2316–2329. http://dx.doi.org/10.1109/TGRS.2009.2012696.

[40] Cao, C., Shao, X., Uprety, S., 2013. “Detecting light outages after severe storms using the SNPP/VIIRS day/night band radiances.” IEEE Geosci. Remote Sens. Lett. 10,1582–1586. http://dx.doi.org/10.1109/LGRS.2013.2262258.

[41] Cao, C., Bai, Y., 2014. “Quantitative analysis of VIIRS DNB nightlight point source for light power estimation and stability monitoring.” Remote Sens. 6, 11915–11935. http://dx.doi.org/10.3390/rs61211915.

[42] Lu, D., et al. (2004) Combination of remote sensing data with socio-economic data to analyze urban expansion and its environmental implications in the Phoenix metropolitan area, USA.

[43] Zeng, X., Shao, X., Qiu, S., Ma, L., Gao, C., Li, C., 2018. “Stability monitoring of the VIIRS day/night band over dome C with a lunar irradiance model and BRDF correction.” Remote Sens. 10, 189.

[44] Lee, S., McIntire, J., Oudrari, H., Schwarting, T., Xiong, X., 2015. “A new method for Suomi-NPP VIIRS day–night band on-orbit radiometric calibration.” IEEE Trans.Geosci. Remote Sens. 53, 324–334. http://dx.doi.org/10.1109/TGRS.2014.2321835.

[45] Liao, L.B., Weiss, S., Mills, S., Hauss, B., 2013. “Suomi NPP VIIRS day-night band on-orbit performance.” J. Geophys. Res. Atmos. 118, 12705–12718. http://dx.doi.org/10.1002/2013JD020475.

[46] Mills, S., Miller, S., 2016. “VIIRS day/night band—correcting striping and non-uniformity over a very large dynamic range.” J. Imaging 2, 9. http://dx.doi.org/10.3390/jimaging2010009.

[47] Levin, N., 2017. “The impact of seasonal changes on observed nighttime brightness from 2014 to 2015 monthly VIIRS DNB composites.” Remote Sens. Environ. 193, 150–164. http://dx.doi.org/10.1016/j.rse.2017.03.003.

[48] Levin, N., Zhang, Q., 2017. “A global analysis of factors controlling VIIRS nighttime light levels from densely populated areas.” Remote Sens. Environ. 190, 366–382. http://dx. Doi.org/10.1016/j.rse.2017.01.006

[49] Bennett, M.M., Smith, L.C., 2017. “Advances in using multitemporal night-time lights satellite imagery to detect, estimate, and monitor socioeconomic dynamics.” Remote Sens. Environ. 192, 176–197. http://dx.doi.org/10.1016/j.rse.2017.01.005.

[50] Miguel O. Romáña, Zhuosen Wangb, Qingsong Sunc, Virginia Kalba, Steven D. Millerd, Andrew Molthanf, Lori Schultze, Jordan Belle, Eleanor C. Stokesg, Bhartendu Pandeyg, Karen C. Setog, Dorothy Hallb, Tomohiro Odah, Robert E. Wolfea, Gary Linj, Navid Golpayegania, Sadashiva Devadigaj,a, Carol Davidsonj, Sudipta Sarkarj, Cid Praderasj, Jeffrey Schmaltzj, Ryan Bollerk, Joshua Stevensj, Olga M. Ramos Gonzálezm, Elizabeth Padillan, José Alonsoo, Yasmín Detrésp, Roy Armstrongp, Ismael Mirandaq, Yasmín Conter, Nitza Marreros, Kytt MacManust, Thomas Eschu, Edward J. Masuokaa.

“NASA's Black Marble nighttime lights product suite”, Remote Sensing of Environment 210 (2018) 113–143

[51] Griggs, D., Stafford-smith, M., Gaffney, O., Rockström, J., Öhman, M.C., Steffen, W., Glaser, G., Kanie, N., Noble, I., 2015. “Policy: sustainable development goals for people and planet.” Nature 495, 5–9. http://dx.doi.org/10.1038/495305a.

[52] http://www.coolgeography.co.uk/Alevel/AQA/Year%2013/Development%20&%20Globalisation/Background/Types%20of%20development.htm

[53] Mahbub ul Haq 1995, “Reflections on Human Development”, Oxford University Press, New York.

[54] Sen, Amartya 1999, “Development as freedom”, Oxford University Press, New York.

[55] Sumayyah Abdul Aziz, Ruzita Mohd Amin, Selamah Abdullah Yusof, Mohamed Aslam Haneef,Mustafa Omar Mohamed & Gapur Oziev, March 2015, “A CRITICAL ANALYSIS OF DEVELOPMENT INDICES”, Australian Journal of Sustainable Business and Society, Volume 01 No. 01

[56] Mthuli Ncube, Charles Leyeka Lufumpa, Victor Murinde, Steve Kayizzi-Mugerwa, “The Africa Infrastructure Development Index (Aidi)”

[57] Julian Donaubauer, Birgit Meyer, Peter Nunnenkamp., June 2014 “A New Global Index of Infrastructure: Construction, Rankings and Applications”, Kiel Working Paper No. 1929, Kiel Institute for the World Economy, Kiellinie 66, 24105 Kiel, Germany

[58] “THE CITY PROSPERITY INITIATIVE, 2015 Global City Report.”, UN-Habitat and International City Leaders, 2015

[59] Maria Emma Santos and Georgina Santos, “Composite Indices of Development”

[60] Infrastructure, Centre for Monitoring Indian Economy (CMIE) (2001), January, 2001,

[61] M.A.C.S.S. Fernando, S. Samita and R. Abeynayake, “Modified Factor Analysis to Construct Composite Indices: Illustration on Urbanization Index”, Tropical Agricultural Research Vol. 23 (4): 327– 337 (2012)

[62] Abhijit Dutta, “Modified poverty index of West Bengal: A human development approach”,Volume 4; Issue 10; October 2017; Page No. 43-50, International Journal of Multidisciplinary Research and Development

[63] Liu, Y., Wang, Z., Sun, Q., Erb, A.M., Li, Z., Schaaf, C.B., Zhang, X., Román, M.O., Scott, R.L., Zhang, Q., 2017. “Evaluation of the VIIRS BRDF, Albedo and NBAR products suite and an assessment of continuity with the long-term MODIS record.” Remote Sens.Environ. 201, 256–274.

[64] Minnis, P., Hong, G., Sun-Mack, S., Smith, W.L., Chen, Y., Miller, S.D., 2016. “Estimating nocturnal opaque ice cloud optical depth from MODIS multispectral infrared radiances using a neural network method.” J. Geophys. Res. Atmos. 121, 4907–4932. http://dx.doi.org/10.1002/2015JD024456.

[65] Walther, A., Heidinger, A.K., Miller, S., 2013. “The expected performance of cloud optical and microphysical properties derived from Suomi NPP VIIRS day/night band lunar reflectance.” J. Geophys. Res. Atmos. 118, 13,230–13,240. http://dx.doi.org/10.1002/2013JD020478.

[66] Charles K. Paul and Adolfo C. Mascarenhas, “Remote Sensing in Development”, 9 October 1981, Volume 214, Number 4517, SCIENCE.

[67] A.A. Belal, F.S. Moghanm , “Detecting urban growth using remote sensing and GIS techniques in Al Gharbiya governorate, Egypt”, The Egyptian Journal of Remote Sensing and Space Sciences (2011) 14, 73–79

[68] Dasika P. Rao, “A Remote Sensing-Based Integrated Approach for

Sustainable Development of Land Water Resources”, IEEE TRANSACTIONS ON SYSTEMS, MAN AND CYBERNETICS—PART C: APPLICATIONS AND REVIEWS, VOL. 31, NO. 2, MAY 2001

[69] C. D. Elvidge1, K. E. Baugh2, S. J. Anderson2,3, P. C. Sutton3, and T. Ghosh2, “The Night Light Development Index (NLDI): a spatially explicit measure of human development from satellite data”, Soc. Geogr., 7, 23–35, 2012, doi:10.5194/sg-7-23-2012

[70] Tilottama Ghosh, Rebecca L. Powell, Christopher D. Elvidge, Kimberly E. Baugh, Paul C. Sutton, Sharolyn Anderson, “Shedding Light on the Global Distribution of Economic Activity”, The Open Geography Journal · January 2010

[71] Douglas Addison,Benjamin Stewart, “Nighttime Lights Revisited: The Use of Nighttime Lights Data as a Proxy for Economic Variables”, Policy Research Working Paper 7496, Macroeconomics and Fiscal Management Global Practice Group, World Bank Group November 2015. DOI: 10.13140/RG.2.1.1526.1200

[72] Shuang Li, Tongyao Zhanga, Zhiyu Yanga, Xi Lib, Huimin Xu, “

NIGHT TIME LIGHT SATELLITE DATA FOR EVALUATING THE SOCIOECONOMICS IN CENTRAL ASIA”, The International Archives of the Photogrammetry, Remote Sensing and Spatial Information Sciences, Volume XLII-2/W7, 2017 ISPRS Geospatial Week 2017, 18–22 September 2017, Wuhan, China

[73] Ran Goldblatta, Michelle F. Stuhlmacherb, Beth Tellmanb, Nicholas Clintonc, Gordon Hansona, Matei Georgescub, Chuyuan Wangb, Fidel Serrano-Candelad, Amit K. Khandelwale, Wan-Hwa Chengb, Robert C. Balling Jrb, “Using Landsat and nighttime lights for supervised pixel-based image classification of urban land cover”, Remote Sensing of Environment 205 (2018) 253–275

[74] Elvidge, C.D., Ziskin, D., Baugh, K.E., Tuttle, B.T., Ghosh, T., Pack, D.W., Erwin, E.H., Zhizhin, M., 2009. A fifteen-year record of global natural gas flaring derived from satellite data. Energies 2, 595–622. http://dx.doi.org/10.3390/en20300595

[75] Zhang, Q., Schaaf, C., Seto, K.C., 2013. The vegetation adjusted NTL urban index: a new approach to reduce saturation and increase variation in nighttime luminosity. Remote Sens. Environ. 129, 32–41. http://dx.doi.org/10.1016/j.rse.2012.10.022

[76] Lu, D., Tian, H., Zhou, G., Ge, H., 2008. Regional mapping of human settlements in southeastern China with multisensor remotely sensed data. Remote Sens. Environ. 112, 3668–3679. http://dx.doi.org/10.1016/j.rse.2008.05.009.

[77] Ma, L., Wu, J., Li, W., Peng, J., Liu, H., 2014. Evaluating saturation correction methods for DMSP/OLS nighttime light data: a case study from China's cities. Remote Sens. 6, 9853–9872. http://dx.doi.org/10.3390/rs6109853.

[78] Huang, X., Schneider, A., Friedl, M.A., 2016. Mapping sub-pixel urban expansion in China using MODIS and DMSP/OLS nighttime lights. Remote Sens. Environ. 175, 92–108. http://dx.doi.org/10.1016/j.rse.2015.12.042.

[79] Jing, W., Yang, Y., Yue, X., Zhao, X., 2015. Mapping urban areas with integration of DMSP/OLS nighttime light and MODIS data using machine learning techniques. Remote Sens. 7, 12419–12439. http://dx.doi.org/10.3390/rs70912419.

[80] Zhang, Q., Li, B., Thau, D., Moore, R., 2015. Building a better urban picture: combining day and night remote sensing imagery. Remote Sens. 7, 11887–11913. http://dx.doi.org/10.3390/rs70911887.

[81] Trianni, G., Lisini, G., Angiuli, E., Moreno, E.A., Dondi, P., Gaggia, A., Gamba, P., 2015. Scaling up to national/regional urban extent mapping using Landsat data. IEEE J. Sel. Top. Appl. Earth Obs. Remote Sens. 8, 3710–3719. http://dx.doi.org/10.1109/JSTARS.2015.2398032.

[82] Kathryn Baragwanath Vogel, Ran Goldblatt, Gordon Hanson, Amit K. Khandelwal. “Detecting urban markets with satellite imagery”, Working Paper, International growth Centre

[83] Michael Xie, Neal Jean, Marshall Burke, David Lobell, and Stefano Ermon, “Transfer Learning from Deep Features for Remote Sensing and Poverty Mapping”, Proceedings of the Thirtieth AAAI Conference on Artificial Intelligence (AAAI-16)

[84] Ryan Engstrom, Jonathan Hersh, David Newhouse, “Poverty from Space: Using High Resolution Satellite Imagery for Estimating Economic Well-being”

[85] Centre for Monitoring Indian Economy (CMIE) (2001). Infrastructure, January, 2001, CMIE, Mumbai.

[86] “Infrastructure for Development”, World Development Report 1994, World Bank.

[87] Charles Leyeka Lufumpa, Maurice Mubila, Fessou Lawson, “The Africa Infrastructure Development Index 2016”, AFDB, May 2016

[88] Susruth Sunder, "Indian Economic Survey 2018: Farmers gain as agriculture mechanization speeds up, but more R&D needed”, financialexpress.com, 29/01/2018

[89] JUAN C. VALDIVIEZO-N, ALEJANDRO TÉLLEZ-QUIÑONES, ADAN SALAZAR-GARIBAY, ALEJANDRA A. LÓPEZ-CALOCA,” Built-up index methods and their applicationsfor urban extraction from Sentinel 2A satellite data: discussion”, Vol. 35, No. 1 / January 2018 / Journal of the Optical Society of America A

[90] Clement Kwang, Edward Matthew Osei Jnr & Adwoa Sarpong Amoah,” Comparing of Landsat 8 and Sentinel 2A using Water Extraction Indexes over Volta River”, Journal of Geography and Geology; Vol. 10, No. 1; 2018